Journal of Photochemistry & Photobiology, A: Chemistry 405 (2021) 112915

Contents lists available at ScienceDirect

Journal of Photochemistry & Photobiology, A: Chemistry

journal homepage: www.elsevier.com/locate/jphotochem

Solid-state solar cells co-sensitized with PbS/CdS quantum dots and N719 dye and based on solid polymer electrolyte with binary cations and nanofillers

M.A.K.L. Dissanayake [a,*], T. Jaseetharan [a,b,c], G.K.R. Senadeera [a,d], B-E. Mellander [e], I. Albinsson [f], M. Furlani [e], J.M.K.W. Kumari [a,b]

[a] National Institute of Fundamental Studies, Hantana Road, Kandy, Sri Lanka
[b] Postgraduate Institute of Science, University of Peradeniya, Peradeniya, Sri Lanka
[c] Department of Physical Sciences, South Eastern University of Sri Lanka, Sammanthurai, Sri Lanka
[d] Department of Physics, The Open University of Sri Lanka, Nawala, Nugegoda, Sri Lanka
[e] Department of Applied Physics, Chalmers University of Technology, Gothenburg, Sweden
[f] Department of Physics, University of Gothenburg, Gothenburg, Sweden

ARTICLE INFO

Keywords:
Solid-state solar cells
Co-sensitization
PbS/CdS quantum dots
N719 dye
Solid polymer electrolyte

ABSTRACT

Co-sensitized solar cells have gained more attention due to the ability of energy conversion process by absorbing photons from wide range of the solar spectrum including visible and near-infrared region. TiO_2 electrodes were co-sensitized with PbS/CdS core-shell quantum dots and N719 dye. PbS/CdS/N719 dye-sensitized solar cells were fabricated with poly(ethylene oxide) based solid polymer electrolyte consisting iodide/triiodide redox couple. The iodide ion conductivity of the electrolyte was enhanced by incorporating a binary iodide salt mixture of different size cations, tetrapropylammonium iodide and potassium iodide. The performance of the solar cell was further enhanced by the incorporating TiO_2 P90 nanofiller in the electrolyte. The best solid-state solar cell showed a significantly higher efficiency of 4.41 % with a short-circuit current density of 8.41 mA cm^{-2}, open-circuit voltage of 748.3 mV and a high fill factor of 70.16 % under the simulated light of 100 mW cm^{-2} with AM 1.5 filter. This is the first report describing the efficiency enhancement in a solid-state dye sensitized solar cell based on a solid polymer electrolyte incorporating a binary cation iodide salt and TiO_2 nanofiller and a photoanode co-sensitized with PbS/CdS quantum dots and N719 dye demonstrating the cumulative effect by the mixed cation effect and co-sensitization.

1. Introduction

Dye-sensitized solar cells (DSSCs) are identified as promising low-cost photovoltaic devices since 1991. These solar cells show better performance under diffuse light compared to the conventional solar cells. Photoelectrode of DSSC consists of a dye-adsorbed porous wide band gap semiconductor layer such as TiO_2, SnO_2 and ZnO [1–4]. Dye molecules absorb light photons and inject electrons to the conduction band of these semiconductors. Several studies have been reported about fabrication and characterization of DSSCs with different dyes as sensitizers including synthetic dyes and natural dyes. However, most of these dyes can capture photons from particular portion of the visible spectrum. In order enhance the light absorption from entire visible and near-infrared (NIR) regions, various studies have been done using near infrared dyes, co-sensitization with different dyes [5–8] and co-sensitization with dye and quantum dots. Single, alloy or core-shell type quantum dots are used for this co-sensitization process.

Semiconductor quantum dots are used for co-sensitization in dye-sensitized solar cells due to their excellent optoelectronic properties such as ability of multiple exciton generation with absorption of single photon, high absorption coefficients, large intrinsic dipole moments and tunable energy gap by quantum confinement effect [9]. Jing Li et al. reported liquid iodide electrolyte based solar cells with a power conversion efficiency of 5.57 %, co-sensitized by CdS quantum dots and N719 dye [10]. In another study, Yanqiong Liu et al. sensitized the TiO_2 electrode with N719 dye and PbS quantum dots in DSSC and enhanced

* Corresponding author.
E-mail address: lakshman.di@nifs.ac.lk (M.A.K.L. Dissanayake).

https://doi.org/10.1016/j.jphotochem.2020.112915
Received 7 June 2020; Received in revised form 6 September 2020; Accepted 11 September 2020
Available online 18 September 2020

the efficiency by 6.72 % [11]. Recently, PbS/CdS/ZnS quantum dots and N719 co-sensitized, cobalt(II/III) redox electrolyte based solar cell has been reported with an efficiency of 2.12 % [12]. In a recent study, CdTe/D719 co-sensitized, iodide/triiodide liquid electrolyte based solar cell has been reported with a high efficiency of 9.17 % [13]. Most of the dye-sensitized solar cells are based on n-type semiconductor. Antonio Carella et al. fabricated novel dyes for p-type dye-sensitized solar cells [14]. Recently, p-type semiconductor-based carbon dots and dye co-sensitized solar cells have been reported by Etefa et al. [15] with a power conversion efficiency of 9.85 %. In their study, dye-sensitized solar cells were fabricated based on composite of NiO with C-dots and N719 dye was used as sensitizer.

Most of the DSSCs were fabricated with liquid electrolytes which may limit the stability of solar cell. Temperature stability of solvent is the major problem in liquid-based electrolyte which contain volatile solvents. Perfect sealing of the cell reduces the evaporation and isolates the electrolyte from the environment [16]. However, at low temperatures, electrolyte may freeze and at high temperatures electrolyte may evaporate or expand and leading to physically damage of the solar cell in large scale fabrication. Optimized perfect sealing is difficult and increases the production cost. Aqueous-based electrolytes have good stability and transparency than the volatile solvent-based electrolytes. Federico Bella et al. reported 100 % water-based dye-sensitized solar cells with an efficiency of 2.5 % [17]. Recently, Metal-free organic dye-sensitized solar cells have been reported with a highest record efficiency of 7.02 %. In this study, iodine-based electrolyte was in 100 % aqueous environment [18].

In order to enhance the stability and prevent the electrolyte leakage of the DSSC, several studies are focusing on the development of quasi-solid (gel type) and solid electrolytes. Polymer based electrolytes have several advantages such as high ionic conductivity, solvent free and flexibility. In quasi-solid electrolytes, polymers and co-polymers are used to reduce solvent leakage and improve the ionic conductivity of the electrolyte [19–21]. Polymer based gel electrolytes are usually synthesized by adding a large amount of liquid plasticizer into a polymer matrix. Gel electrolytes have relatively high ambient ionic conductivity and poor mechanical properties than the pure polymer electrolytes. Solid-state DSSCs have been fabricated with polymers, co-polymers, organic and inorganic hole transporting materials such as CuI, CuSCN and Spiro-MeOTAD [21–24]. Solid polymer electrolytes are gaining more attention in the fabrication of solar cells and rechargeable batteries due to the ease of fabrication and excellent properties such as electrochemical stability with solvent-free condition and high ionic conductivity [25]. Hongwei Han et al. reported dye-sensitized solar cell based on poly(ethylene oxide)/poly(vinylidene fluoride) based solid co-polymer electrolyte with an efficiency of 4.8 % [26]. In another study, poly(ethylene oxide)/poly(propylene glycol) solid polymer electrolyte based DSSC has been reported with a power conversion efficiency of 3.84 % by Moon-Sung Kang et al. [27]. Recently, Sundaramoorthy et al. reported 4,4′-bipyridine-doped poly(vinylidene fluoride) solid polymer electrolyte DSSC with an efficiency of 4.4 % [28]. In a recent study, polyaniline-thiourea based solid polymer electrolyte has been reported with 73 % enhancement of overall efficiency [29]. Solid-state dye-sensitized solar cells have been fabricated and characterized with poly(ethylene oxide)/polyaniline electrolytes by Duan et. al. [30].

Efficiency of polymer based quasi-solid state and solid state DSSCs have been enhanced by optimizing the size of the cation and introducing suitable different size binary cations in to the electrolyte. Effect of cation size on solid polymer electrolyte based DSSC has been reported [31]. In another study, polyacrylonitrile (PAN) based gel electrolyte with mixed cation has been reported with an efficiency of 5.36 % [32]. Arof et al. reported the effect of mixed cations in polyvinylidene fluoride (PVdF) polymer electrolyte based DSSC with 3.92 % efficiency [33]. Among the polymers, PEO is important for the preparation of solid polymer electrolytes and it has mechanical flexibility, corrosion resistance and can easily solvate ions [34]. In order to enhance the efficiency of the polymer based DSSC, nanofillers such as TiO_2 nanoparticles were introduced in polymer electrolytes [35,36]. Stability of liquid, quasi-solid-state, and solid-state electrolytes in quantum dot-sensitized solar cell applications were discussed by Duan et.al. [37].

In the present study, TiO_2 electrodes were sensitized with PbS/CdS quantum dots and N719 dye. Co-sensitization was done with successive ionic layer adsorption and reaction (SILAR) method and solid state DSSCs have been fabricated with poly(ethylene oxide) (PEO) based iodide electrolyte. The efficiency of the solar cells has been further enhanced by introducing binary cations in the iodide electrolyte. Tetrapropylammonium iodide was gradually replaced by potassium iodide and the optimum ratio has been determined corresponding to the high efficiency. TiO_2 P90 nanoparticles have been introduced in to the electrolyte and the amount of P90 nanoparticle for high efficiency of the solar cell has been optimized. Thermal, electrical and optical properties of the PEO based solid electrolyte have been studied.

2. Experimental

TiO_2/PbS/CdS/N719 electrodes have been fabricated and optical and morphology characterizations were done. PEO based gel electrolytes were fabricated with different ratios of binary salts and TiO_2 nanofiller. Electrical and thermal characterizations of each electrolytes were done. In order to fabricate the solid polymer electrolyte, the solvent evaporation time and temperature were optimized. All solid-state solar cells were characterized under the same standard conditions.

2.1. Materials

Poly(ethylene oxide) (Mw = 400000, Aldrich), tetrapropylammonium iodide (98 %, Aldrich), potassium iodide (99.5 %, Sigma-Aldrich), iodine (98.8 %, Sigma-Aldrich), sodium sulfide hydrate (>60 %, Sigma-Aldrich), cis-diisothiocyanato-bis(2,2′-bipyridyl-4,4′-dicarboxylato) ruthenium(II) bis(tetrabutylammonium) (N719 dye, Solaronix), Triton X-100 (Sigma-Aldrich), poly(ethylene glycol) (MW = 1000, 99.8 %, Sigma-Aldrich), lead (II) nitrate (99 %, Sigma-Aldrich), cadmium chloride (99 %, Alfa Aesar), titanium dioxide P25 powder (Degussa), titanium dioxide P90 powder (Evonik, Germany), fluorine-doped tin oxide (FTO) coated glass (8 Ω cm^{-2}, Solarnoix). tetrapropylammonium iodide, potassium iodide and poly(ethylene oxide) were vacuum-dried for 24 h prior to use and all other chemicals were used as received without further purification.

2.2. Preparation of TiO_2 electrode

1 cm × 2 cm FTO glass substrates were cleaned according to the standard cleaning process. 0.25 g of TiO_2 P90 powder and 1 mL of 0.1 M HNO_3 were mixed and crushed until a creamy paste was obtained. The paste was deposited on the conducting side of FTO glass by spin coating process with 3000 rpm for 1 min and the electrodes were sintered at 450 °C for 45 min. These compact layer electrodes were allowed to reach room temperature. For the fabrication of the TiO_2 P25 nanoparticles paste, 0.25 g of TiO_2 P25 powder were grounded with 0.5 mL of 0.1 M HNO_3 and one drop of triton X-100 was added to the paste and mixed. Finally, 0.05 g of PEG 1000 and 0.5 mL of 0.1 M HNO_3 were added to the paste and grounded. Grinding process was continued until the paste became creamy. The P25 paste was applied on the P90 layer by doctor blade technique and the FTO/TiO_2 P90/TiO_2 P25 electrodes were sintered at 450 °C for 45 min. Electrodes were allowed to cool slowly and 5 mm × 5 mm area was selected and TiO_2 layer was removed from other area. Active area of the TiO_2 electrode was 0.25 cm^2. In order to study the co-sensitization of PbS/CdS quantum dots and N719 dye, two types of N719 dye-adsorbed electrodes were fabricated with and without PbS/CdS quantum dots.

2.3. Deposition of PbS/CdS quantum dots

Incorporation of quantum dots were done by successive ionic layer adsorption and reaction (SILAR) technique. 0.1 M $Pb(NO_3)_2$ and 0.1 M Na_2S in de-ionized water were used as the cationic and anionic sources, respectively, for the deposition of PbS quantum dots. 0.1 M $CdCl_2$ and 0.1 M Na_2S in de-ionized water were used as cationic and anionic precursor solutions for CdS quantum dots. Dipping time for each precursor solution was kept at 1 min. In order to fabricate good photoanode, the SILAR cycles were optimized by fabricating solar cells. For the fabrication of FTO/TiO_2/PbS/CdS photoelectrode, one and three SILAR cycles were done for the deposition of PbS and CdS quantum dots, respectively.

In order to prepare the cationic precursor solution, $CdCl_2$ was dissolved in deionized water. In this process, the solution was ultrasonicated until all the $CdCl_2$ were dissolved. The size of the CdS quantum dots depends on the concentration of the precursor solution, dipping time and number of SILAR cycles. In this study, the size of the quantum dots were controlled by controlling the number of SILAR cycles.

2.4. Co-sensitization with dye

In order to prepare FTO/TiO_2/PbS/CdS/N719 photoanode, FTO/TiO_2/PbS/CdS electrodes were dipped in to 0.3 mM of N719 ethanolic solution for 24 h at room temperature. Then, the photoanodes were washed with ethanol to remove excess dye molecules.

2.5. Preparation of PEO – based gel electrolytes

0.1564 g of tetrapropylammonium iodide (Pr_4NI) and 0.0158 g of iodine were dissolved in 1.5 mL of acetonitrile and the solution was stirred at room temperature until all solid compositions completely dissolved. 0.264 g of PEO were added to the solution and the solution was continuously stirred for 12 h to get homogeneous gel electrolyte. In order to compare the effect of mixed cations and nanofiller in the electrolyte, three different types of PEO based electrolytes were fabricated and the number of iodide mole was kept constant in each type electrolyte.

1) PEO + I_2 + Pr_4NI
2) PEO + I_2 + KI
3) PEO + I_2 + Pr_4NI + KI

For the preparation of mixed cation-based polymer electrolyte, Pr_4NI was gradually replaced by potassium iodide and the total mole of iodide was kept constant. A series of electrolytes (a–h) with different molar ratio of mixed cations were synthesized according to Table 1.

Finally, a series of non-flowing gel electrolyte samples were obtained as shown in Fig. 1. The best solid electrolyte composition was identified by the conductivity measurements of the electrolyte and photovoltaic measurements of the solar cells.

Table 1
Salt compositions of the PEO based electrolytes.

Electrolyte	Molar percentage of Pr_4NI (%)	Molar percentage of KI (%)	Amount of Pr_4NI (g)	Amount of KI (g)
a	100	0	0.1564	0
b	90	10	0.1408	0.0083
c	80	20	0.1251	0.0166
d	70	30	0.1095	0.0249
e	60	40	0.0938	0.0332
f	40	60	0.0626	0.0497
g	20	80	0.0313	0.0663
h	0	100	0	0.0829

2.6. Nanofiller effect in electrolyte

In order to enhance the conductivity of the electrolyte by nanofillers, different weight percentages (2.5 %, 5%, 7.5 % and 10 % of the PEO) of TiO_2 P90 nanoparticles were added to the best mixed cation-based polymer electrolyte separately and the electrolytes were magnetically stirred until a homogeneous mixture was obtained.

2.7. Fabrication of solid state PbS/CdS/N719 solar cells

An appropriate amount of gel-like polymer electrolyte was applied on the active side of the photoanode. The gel like nature due to the presence of the minimum quantity of acetontrile helps the polymer electrolyte to penetrate adequately into the nanoporous TiO_2 surface. Pt counter electrode was placed on the electrolyte and both electrodes were held under gentle pressure using two stainless steel clips. In order to completely remove the acetonitrle solvent from the electrolyte, assembled solar cells were vacuum dried at 55 °C for 2.5 h. The absence of even traces of acetonitrile from the electrolyte after vacuum drying was confirmed using an electrolyte sample removed from a similarly assembled and vacuum dried duplicate solar cell with the help of FTIR spectroscopy.

2.8. Optical absorption measurements

In order to understand the contribution of the PbS/CdS quantum dots to the optical absorption of the photoanode, optical absorption spectra of the TiO_2 electrode, N719 dye - adsorbed TiO_2 electrode and TiO_2 electrode co-sensitized with PbS/CdS quantum dots and N719 dye were obtained by Shimadzu 2450 Spectrophotometer in the wavelength range between 350 nm and 1100 nm.

2.9. Transmission electron microscopy (TEM) and EDX spectroscopy analysis

Size and shape of the were analyzed by using JEOL-2100 high-resolution transmission electron microscope (HRTEM) with an accelerating voltage of 200 kV. Elemental composition of the PbS/CdS quantum dot-sensitized TiO_2 electrodes were analyzed using Ametek EDAX module with Octane T Optima-60 EDX detector in transmission electron microscopic mode.

2.10. Fourier transform infrared (FTIR) spectroscopy measurements

Acetonitrile was used as the solvent for the synthesis of PEO based gel electrolyte. In order to confirm the absence of the acetonitrile, FTIR spectroscopy was obtained for the synthesized PEO based gel and solid-state polymer electrolytes by using Bruker Alpha FTIR spectrometer with Platinum ATR module.

2.11. Differential scanning calorimetry measurements

Differential scanning calorimetry (DSC) measurements of the solid polymer electrolyte films were done by using Mettler Toledo DSC 30 differential scanning calorimeter with Mettler TC10A/TC15 controller. 40 μL Al crucibles were used as reference and sample container. Heating rate was 10 ℃/min with temperature range between -122 ℃ and 80 ℃.

2.12. Temperature dependent ionic conductivity measurements

Ionic conductivities of the solid polymer electrolytes were studied from complex impedance data of the electrolytes. Complex impedance measurements were done by using Agilent E4980A precision LCR meter with a frequency range between 20 Hz and 2 MHz. Solid polymer electrolyte film was sandwiched between two polished stainless-steel electrodes. All measurements were carried out between 10 ℃ and 80

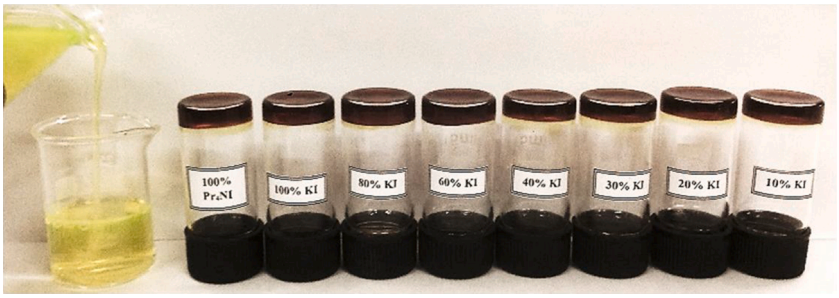

Fig. 1. Synthesized non-flowing gel electrolytes in inverted bottles. The gel nature of the electrolytes was due to the acetonitrile present in the system.

 with 10 ℃ intervals. In order to maintain the steady temperature, the sample holder was kept in water bath coupled with Hetofrig/Grant cooling-heating system.

2.13. Current – voltage characterization

In order to compare the power conversion efficiencies of the solar cells, photocurrent - voltage measurements of the solar cells were done using a computer-controlled multimeter (Keithley 2000 model) coupled with potentiostat/galvanostat unit (HA-301) under simulated light of 100 mW cm^{-2} with AM 1.5 spectral filter. Active area of the fabricated solar cell was 0.25 cm^2. For each electrolyte composition, at least five different solar cells were fabricated and their I–V characteristics were measured. When calculating, the average value of the efficiencies were noted along with corresponding errors.

2.14. Electrochemical impedance spectroscopy (EIS) measurements

Interface resistances and electrochemical capacitances of the solar cell can be obtained from electrochemical impedance spectroscopy. EIS measurements of each solar cells were done under the simulated light of 100 mW cm^{-2} with AM 1.5 filter by using Autolab (Metrohm) potentiostat/galvanostat PGSTAT128 N with an FRA 32 M with an ac amplitude of 10 mV and the bias potential was equal to the open-circuit voltage of the solar cell. EIS was recorded over a frequency range between 10 mHz and 1 MHz. Series resistance and interface resistances were calculated by fitting a suitable equivalent circuit with obtained data.

3. Results and discussion

3.1. Optical absorption

Fig. 2(i) depicts the absorption spectra of (a) TiO_2 electrode, (b) TiO_2 electrode sensitized with N719 dye and (c) TiO_2 electrode co-sensitized with PbS/CdS quantum dots and N719 dye. Dye-sensitized photoanode shows a broad absorption peak in the visible region between 500 nm and 560 nm (curve (b)). This peak clearly confirms the adsorption of the N719 dye on TiO_2 electrode. Photoanode co-sensitized with PbS/CdS quantum dots and N719 shows a broad absorption in the visible region between 450 nm and 700 nm (curve (c)). This feature clearly indicates the contribution from both N719 dye and CdS quantum dots in the absorption of visible photons [38,39]. Peak of the curve (c) is blue shifted due to the absorption CdS quantum dots. This photoanode displays another clear peak around 900−1100 nm, which is in the near infrared region due to the strong absorption by the PbS quantum dots [40]. Co-sensitization with PbS/CdS quantum dots in the photoanode shows more obvious enhancement of the absorption in the entire visible region and near infrared region of the solar spectrum.

Fig. 2(ii) shows the absorption spectrum of N719 dye solution which was used in this study. It clearly shows the dominant broad absorption peak at 525 nm wavelength.

3.2. TEM and EDX analysis

Fig. 3 (a) and (b) show the TEM and HRTEM images of PbS/CdS quantum dots-sensitized TiO_2, respectively. According to the number of SILAR cycles, PbS/CdS quantum dots did not cover the entire TiO_2 and there is enough space for N719 dye adsorption. Average sizes of the quantum dots between 3.5 nm and 10 nm.

Fig. 4 and Fig. 5 display the EDX spectrum and elemental maps of the PbS/CdS quantum dot-sensitized TiO_2. It clearly confirms the existence of Pb and Cd in TiO_2 with correct atomic composition, which depends on the number of SILAR cycles.

3.3. FTIR spectroscopy

Fig. 6 displays the FTIR spectra of the gel and solid phases of the PEO based electrolytes. Acetonitrile was used as the solvent to synthesize the gel polymer electrolyte. In order to get a solid electrolyte, the electrolyte was vacuum dried for different time durations and different temperatures. Vacuum drying temperature and time were optimized with obtained FTIR spectra from the ATR technique. FTIR spectrum of the gel type electrolyte (curve 1) shows a sharp peak around 2254 cm^{-1}, which

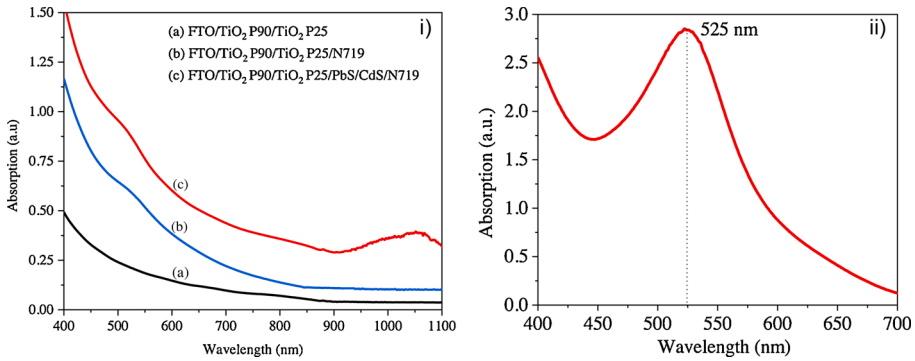

Fig. 2. (i) Optical absorption spectra of the TiO_2 electrode and co-sensitized photoanodes. (ii) The optical absorption spectrum of the N719 dye solution.

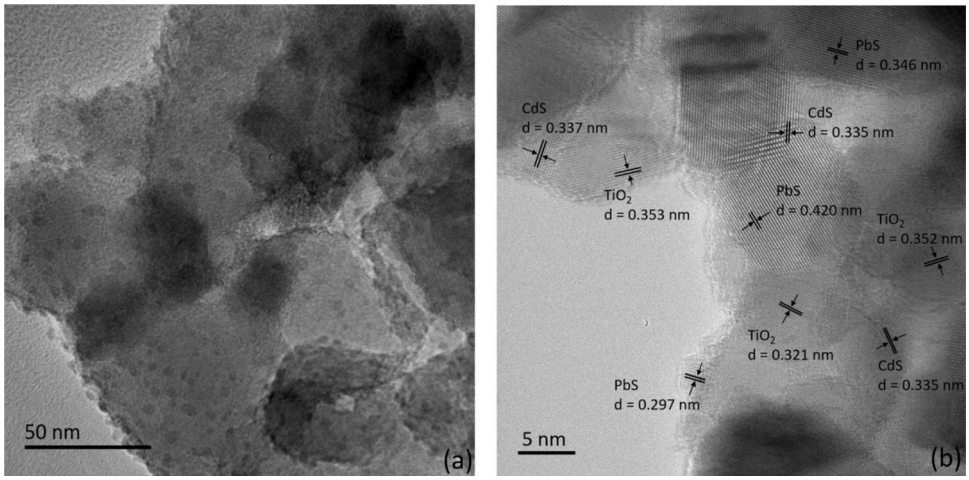

Fig. 3. (a) TEM, (b) HRTEM images of PbS/CdS quantum dots-sensitized TiO_2.

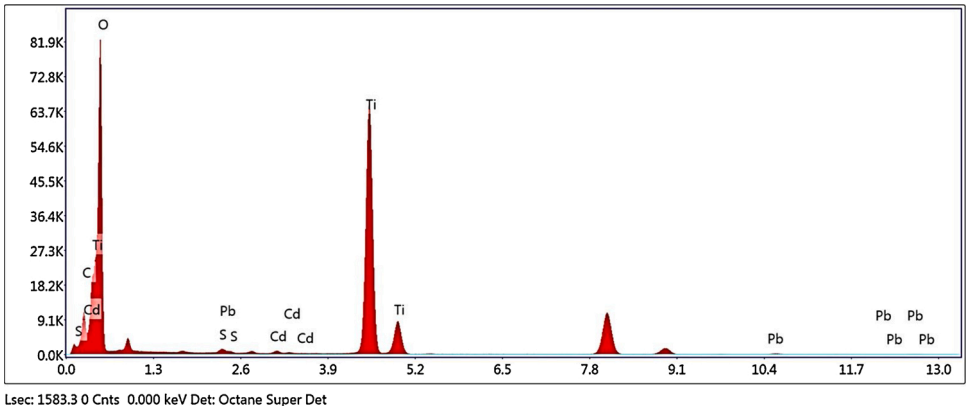

Fig. 4. EDX spectrum of PbS/CdS quantum dots-sensitized TiO_2.

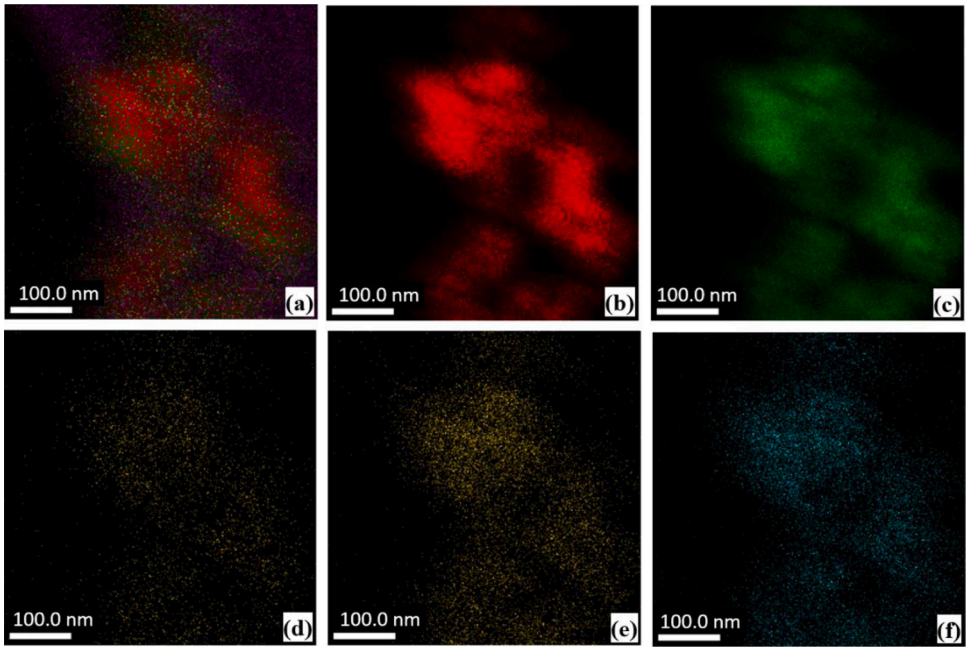

Fig. 5. Elemental mapping of (a) selected area (b) Ti, (c) O, (d) Pb, (e) Cd and (f) S.

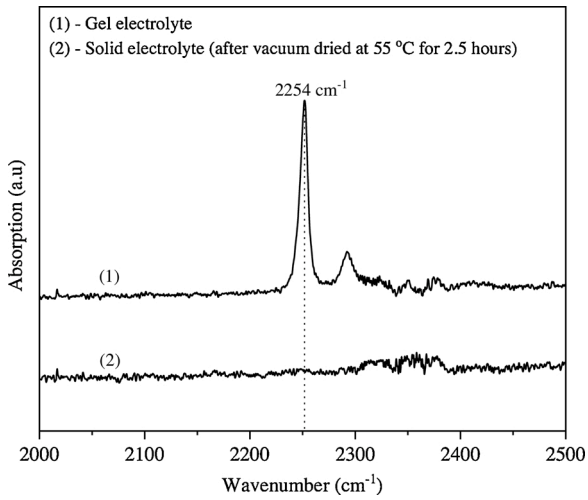

Fig. 6. FTIR spectra of the gel polymer electrolyte and solid polymer electrolyte.

corresponds to the $C \equiv N$ stretching mode of the acetonitrile [41,42]. After the vacuum drying at 55 ℃ for 2.5 h, acetonitrile was completely evaporated from the electrolyte and the electrolyte became a solvent-free solid electrolyte. Absence of acetonitrile was confirmed by the FTIR spectrum of the solid electrolyte (curve 2).

3.4. Differential scanning calorimetry (DSC) analysis

Fig. 7 displays the DSC traces of the pure PEO and different PEO based solid electrolytes with optimized amount of Pr_4NI, KI and TiO_2 P90 nanofiller. Pure PEO shows an endothermic peak around 68.6 ℃ and the melting temperature of PEO decreases due to the addition of Pr_4NI and KI salts. This nature of the PEO/salt system is in agreement with those described in the literature [43–45]. Melting temperature of the PEO based electrolyte further decreases due to the addition of suitable amount of TiO_2 P90 nanofillers. Several nanofillers show similar effects in the polymer electrolytes [46–48]. Degree of crystallinity gives the fraction of the crystalline and amorphous phases of the electrolyte. Degree of crystallinity (χ_c) of synthesized different solid electrolyte compositions were calculated using the following equation:

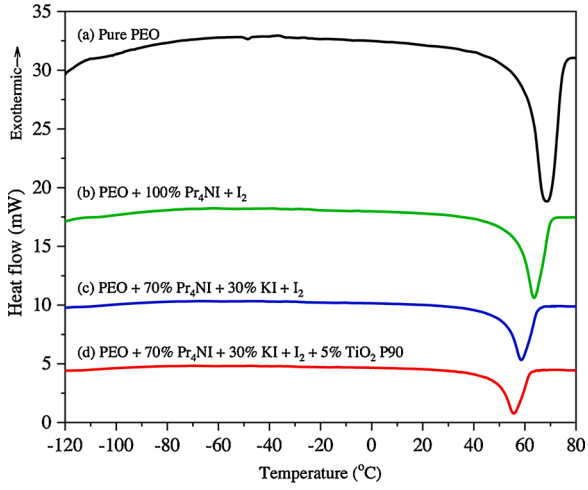

Fig. 7. DSC traces of (a) pure PEO; (b) PEO with optimized amount of Pr_4NI salt; (c) PEO with optimized amount of mixed salt of Pr_4NI and KI; (d) PEO with optimized mixed salts and TiO_2 P90 nanofiller.

$$\chi_c = \frac{\Delta H^f}{\Delta H_f^o} \times 100\%$$

Here, ΔH_f^o is the melting enthalpy of fusion of 100 % pure crystalline PEO, which is equal to 213.7 J g^{-1} [49,50] and ΔH^f denotes by the melting enthalpy of the solid polymer electrolyte calculated using the DSC traces.

Melting temperatures (T_m) and estimated values of the crystallinities are listed in Table 2. Crystallinity of PEO is reduced from 88.74 % to 47.51 % due to the addition of Pr_4NI salt and further reduced by KI and reached up to 32.14 %. This is caused by the destruction of the regular crystalline network of PEO by the salts. A remarkable reduction has been observed in the crystallinity of the solid polymer electrolyte by the addition of TiO_2 P90 nanofillers. High crystallinity of the polymer in the electrolytes leads to lower ionic mobility, which directly affects the photocurrent of the solar cell. Addition of appropriate amounts of binary salts and semiconductor nanofillers increases the amorphous phase of the PEO based electrolyte and enhances the ionic transport as reported in previous studies [47,48,51]. Crystallinity of the PEO is decreased by 63.8 % by the mixed salt combination of 70 % Pr_4NI + 30 % KI and it is further reduced by 15 % due to the addition of TiO_2 P90 nanofillers. This significant reduction of the crystalline phase of the electrolyte facilitates the ionic motion of the ions in the polymer matrix and enhances the photocurrent performance of the solar cells.

3.5. Ionic conductivity of the solid electrolytes

Ionic conductivity (σ) of the solid electrolyte films in different temperature can be calculated using the following equation:

$$\sigma = \frac{L}{R_b A}$$

L and A are the thickness and cross-section area of the electrolyte film and R_b is the bulk resistance of the electrolyte which was calculated from the complex impedance plot. Temperature dependence of ionic conductivity has been studied using the following Arrhenius equation:

$$\sigma T = B \exp\left(\frac{-E_a}{k_b T}\right)$$

where E_a is the activation energy, k_B is the Boltzmann constant and B is a constant called the pre-exponential factor.

Fig. 8 shows the variation of $\ln(\sigma T)$with inverse of the absolute temperature of the solid electrolyte films with different amount of Pr_4NI and KI. Increase in ionic conductivity with the amount of salts is attributed to the increment in amorphous phase in the electrolyte. Increasing amorphous phase increases the free volume and it facilitates the motion of the ions. Ionic conductivity gradually increases due to the addition of KI in to the mixed cation electrolyte and highest conductivity was found corresponding to the electrolyte (h), which contains 100 % of KI salt. Pr_4N^+ cation is larger than K^+ cation and K^+ ions are expected to be high mobility in in the electrolyte compared to Pr_4N^+ ions as described in the previous reports on gel polymer electrolytes [36,52,53]. However, highest power conversion efficiency of the solar cell was obtained for the electrolyte (d), which contains mixed salt of 70 % Pr_4NI

Table 2
Parameters calculated from DSC measurements of different electrolyte compositions.

Electrolyte	T_m (°C)	ΔH^f ($J\,g^{-1}$)	χ_c(%)
Pure PEO	68.6	189.64	88.74
PEO + 100 % Pr_4NI + I_2	63.9	101.52	47.51
PEO + 70 % Pr_4NI + 30% KI + I_2	58.5	68.69	32.14
PEO + 70 % Pr_4NI + 30% KI + I_2 + 5% TiO_2 P90	55.7	58.37	27.31

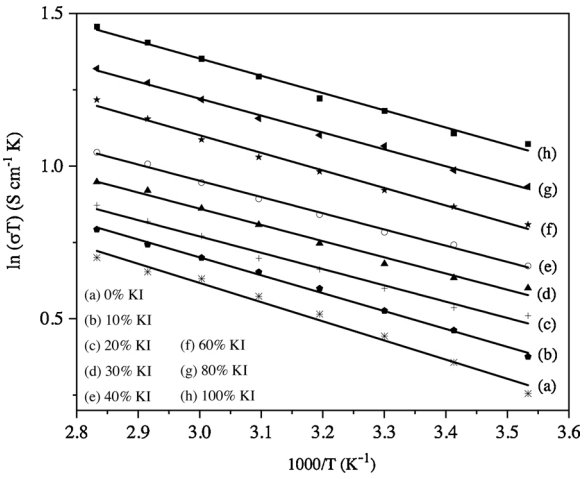

Fig. 8. Variation of ln(σT) with inverse of the absolute temperature for the PEO based solid electrolyte films with different molar percentage of KI.

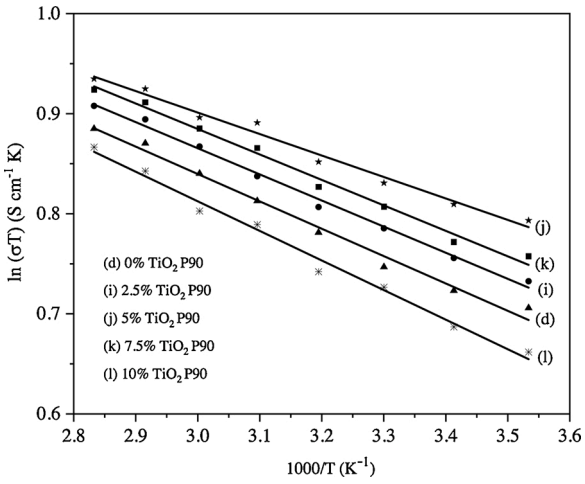

Fig. 9. Variation of ln(σT) with inverse of the absolute temperature for the PEO based solid electrolyte films with different amount of TiO_2 P90 nanofiller.

and 30 % KI. Higher conductivity of the electrolyte comes from the higher mobility of K^+ ions, these are not contributing to the performance of the solar cell.

Activation energy values of the different solid electrolytes were calculated from the gradients of linear fit of the Arrhenius plots and the activation energy values are recorded in Table 3. Activation energy values decrease with increasing concentration of KI [53,54].

Fig. 9 shows the variation of $\ln(\sigma T)$with the inverse of the absolute temperature of the solid electrolyte films with different weight percentages of TiO_2 P90 nanofiller. Ionic conductivity of the electrolyte increases with the amount of the TiO_2 P90 nanofiller and gets a high conductivity corresponding to 5% nanofiller. Increase in the conductivity is due to the reduction of crystalline phase and degree of aggregation within the polymer-salt mixture [52,55,56]. Further addition of nanofiller more than 5% makes a decrement in the ionic conductivity. More TiO_2 P90 nanofillers decreases the free volume and flexibility of the polymer electrolyte.

Value of activation energies with the amount of nanofiller is listed Table 4. Activation energy decreases with increasing the amount of nanofiller and a minimum value was observed corresponding to the 5% of TiO_2 P90 nanofiller. Further addition of nanofiller increases the activation energy and leads to decrease the performance of the electrolyte as well as the efficiency of the solar cell.

3.6. Photovoltaic performance of the solar cells

Current – voltage characterizations of solar cells fabricated with PEO based solid polymer electrolyte were obtained under the simulated light of 100 mW cm^{-2} with AM 1.5 spectral filter. Fig. 10 shows the photovoltaic performance of the solid polymer electrolyte (PEO + Pr_4NI + I_2) based solar cells with N719 dye-sensitized photoanode and photoanode co-sensitized with PbS/CdS quantum dots and N719 dye. Co-sensitized solar cell shows a better efficiency of 3.54 %, while solar cell sensitized with dye alone shows an efficiency of 2.94 %. Short-circuit current density increases from 5.34 mA cm^{-2} to 6.38 mA cm^{-2}. This clearly shows that the enhancement in the short-circuit photocurrent is due to the PbS/CdS core-shell quantum dots.

Effects of mixed cation concentration on the photovoltaic parameters are summarized in Table 5. Short-circuit current density and overall efficiency gradually increase with the amount of KI and show a highest efficiency of 4.22 % with a short-circuit current density of 7.15 mA cm^{-2} corresponding to the composition of 70 % Pr_4NI and 30 % KI. However,

Table 3
Calculated activation energy values of the electrolyte with different amount of KI.

Solid electrolyte	Molar percentage of Pr_4NI (%)	Molar percentage of KI (%)	Activation energy (eV)
a	100	0	0.346
b	90	10	0.319
c	80	20	0.306
d	70	30	0.291
e	60	40	0.289
f	40	60	0.284
g	20	80	0.279
h	0	100	0.277

Table 4
Calculated activation energy values of the electrolyte with different amount of TiO_2 P90 nanofiller.

Electrolyte	Composition	E_a (eV)
d	PEO + I_2+ 70% Pr_4NI + 30% KI	0.291
i	PEO + I_2+ 70% Pr_4NI + 30% KI + 2.5% TiO_2 P90	0.286
j	PEO + I_2+ 70% Pr_4NI + 30% KI + 5% TiO_2 P90	0.275
k	PEO + I_2+ 70% Pr_4NI + 30% KI + 7.5% TiO_2 P90	0.291
l	PEO + I_2+ 70% Pr_4NI + 30% KI + 10% TiO_2 P90	0.313

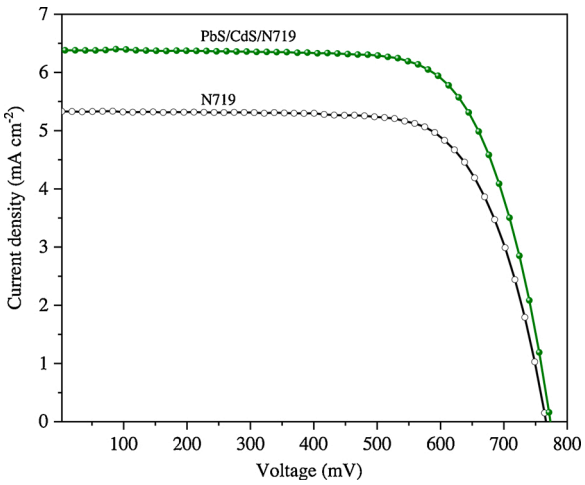

Fig. 10. Current – voltage characterization of solid polymer solar cells with different photoanodes under the illumination of 100 mW cm^{-2} with AM 1.5 spectral filter.

Table 5
Mixed cation effect on photovoltaic parameters of the solar cells under the illumination of 100 mW cm^{-2} with AM 1.5 spectral filter.

Electrolyte	Pr_4NI:KI (mol %)	V_{OC} (mV)	J_{SC} (mA cm^{-2})	FF (%)	Efficiency (%)
a	100:0	773.0	6.380	71.83	3.54 ± 0.12
b	90:10	760.0	6.628	72.18	3.64 ± 0.15
c	80:20	757.9	7.152	71.39	3.87 ± 0.15
d	70:30	749.9	7.996	70.43	4.22 ± 0.19
e	60:40	743.6	7.432	69.81	3.83 ± 0.14
f	40:60	726.6	7.148	68.33	3.54 ± 0.14
g	20:80	718.6	6.764	67.76	3.29 ± 0.13
h	0:100	690.0	6.524	68.70	3.09 ± 0.09

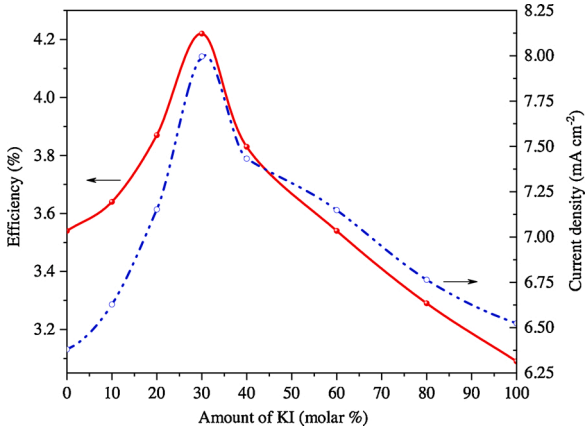

Fig. 11. Variation of efficiency (solid line) and short-circuit current density (dotted lines) with KI under the illumination of 100 mW cm^{-2} with AM 1.5 spectral filter.

the open-circuit voltage is gradually reduced by the addition of KI. Further addition of KI reduces the efficiency. Fig. 11 shows the variation of the efficiency and short-circuit current density with the amount of KI. Both curves show same features, clearly showing that increase in the efficiency is attributed the enhanced photocurrent density due to the mixed cation effect [32,36].

Effect of the TiO_2 P90 nanofiller has been studied with the best combination of mixed cation (70 % Pr_4NI and 30 % KI) based solid polymer electrolyte. Variation of the photovoltaic parameters of the solar cells made with solid electrolytes with different amount of TiO_2 P90 nanofiller are listed in Table 6. Short-circuit current density increases due to the addition of nanofiller and shows a higher value of 8.412 mA cm^{-2} corresponding to the 5% of the nanofiller. Further addition of nanofiller above 5% reduces the current density due to the reduction of the mobility of the ions, evidently due to the blocking effect.

Fig. 12 displays the current – voltage characteristics of the PbS/CdS/N719 co-sensitized solar cells fabricated with PEO based solid electrolyte having mixed iodide salts and TiO_2 nanofillers. All solid-state solar cells show better and nearly equal fill factor values, this indicates the

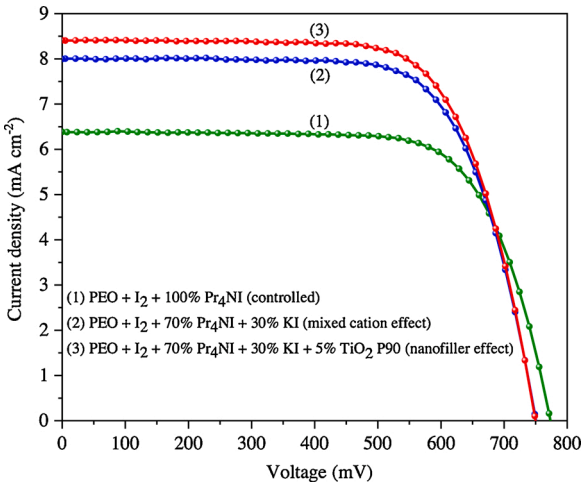

Fig. 12. Current – voltage characterization of PbS/CdS/N719 co-sensitized solar cells with different PEO based solid electrolyte compositions under the illumination of 100 mW cm^{-2} with AM 1.5 spectral filter.

good surface contacts between the electrodes and solid polymer electrolyte interface. Current density of the solar cell is enhanced by mixed cation effect in the electrolyte (curve 2) and it is further enhanced by the nanofiller effect (curve 3). Short-circuit current density shows 1.6-fold increase, while the open-circuit voltage is decreased by 23 mV. The enhancement of the short-circuit current density is due to the mixed cation effect by different size cations [32,36,53].

Photovoltaic parameters of the best optimized solar cells are listed in Table 7. Efficiency of the controlled solar cell corresponding to the 100 % Pr_4NI salt in the electrolyte shows an efficiency of 3.54 %. The overall efficiency of the solar cell is increased by more than 19 % due to the mixed cation effect in the electrolyte and the efficiency of the solar cell is further increased by 4.50 % through the nanofiller effect in the electrolyte. Nanofiller enhances the ionic conductivity through the reduction of crystallinity of the electrolyte medium and further addition of nanofiller reduces the ion mobility due to the blocking effect as described in the previous reports [36,52,55].

A comparison of the efficiency of best DSSC electrolyte used in this work with the efficiencies of the best PEO solid polymer electrolyte based DSSC and a non-polymer based, novel electrolyte, C2v-symmetric spiro-configured HTM-1 (perovskite solar cell) is given in Table 8. This comparison shows that higher efficiencies can be achieved with PEO based solid polymer electrolytes using various additives and ionic liquids and using other types of solid electrolytes such as spiro-based hole transport materials, which needs complex and expensive chemicals and special environments to fabricate.

3.7. EIS analysis of the solar cells

Electrochemical impedance data were analyzed by fitting a suitable equivalent circuit and the series resistance and interfacial resistances were determined. Fig. 13 shows the Nyquist plots of the controlled solar

Table 6
Nanofiller effect on photovoltaic parameters of the solar cells under the illumination of 100 mW cm^{-2} with AM 1.5 spectral filter.

Amount of TiO_2 P90 nanofiller (wt % of PEO)	V_{OC} (mV)	J_{SC} (mA cm^{-2})	FF (%)	Efficiency (%)
0	749.9	7.139	70.43	4.22 ± 0.16 0.06
2.5	749.1	8.388	68.75	4.32 ± 0.18
5	748.3	8.412	70.16	4.41 ± 0.18
7.5	742.3	6.836	6.96	3.55 ± 0.14
10	738.5	5.700	70.61	2.97 ± 0.11

Table 7
Summary of the photovoltaic parameters of the best PEO solid polymer electrolyte based solar cells with the mixed cation effect and nanofiller effect.

Optimized compositions of solid polymer electrolyte	V_{OC} (mV)	J_{SC} (mA cm^{-2})	FF (%)	Efficiency (%)
(1) PEO + I_2 + 100% Pr_4NI (reference)	773.0	6.380	71.83	3.54 ± 0.06
(2) PEO + I_2 + 70% Pr_4NI + 30% KI	749.9	7.996	70.43	4.22 ± 0.11
(3) PEO + I_2 + 70% Pr_4NI + 30% KI + 5% TiO_2 P90	748.3	8.412	70.16	4.41 ± 0.09

Table 8
Comparison of best solar cell efficiency with other reported best solid state DSSC efficiencies.

Solid Electrolyte	Efficiency (%)	References
PEO + I_2 + 70% Pr_4NI + 30% KI + 5% TiO_2 P90 (PEO based solid electrolyte with no additives)	4.41 ± 0.09	This work
PEO+ 2.0 M 1- methyl-3-propylimidazolium iodide (MPII)+ 0.8 M I_2, 0.1 M KI + 0.5 M TBP, PEGDME (PEO based solid electrolytes with additives and ionic liquid)	8.20	**Ref** [[59]]: Woohyung Cho, Young Rae Kim, Donghoon Song, Hyung Woo Choi and Yong Soo Kang; J. Mater. Chem. A, **2014**, 2, 17,746
Cyclopentadithiophene-based symmetric spiro-configured Hole-Transporting MateriaHTM-1 Perovskite solar cell electrolyte (A state of the art, latest non-polymer based, electrolyte)	21	**Ref [** [60]]: Seckin Akin, Michael Bauer, Ryusuke Uchida, Neha Arora, Gwenole Jacopin, Yuhang Liu, Dirk Hertel, Klaus Meerholz, Elena Mena-Osteritz, Peter Bäuerle, Shaik Mohammed Zakeeruddin, M Ibrahim Dar, Michael Grätzel ACS Applied Energy Materials **2020**/7/6

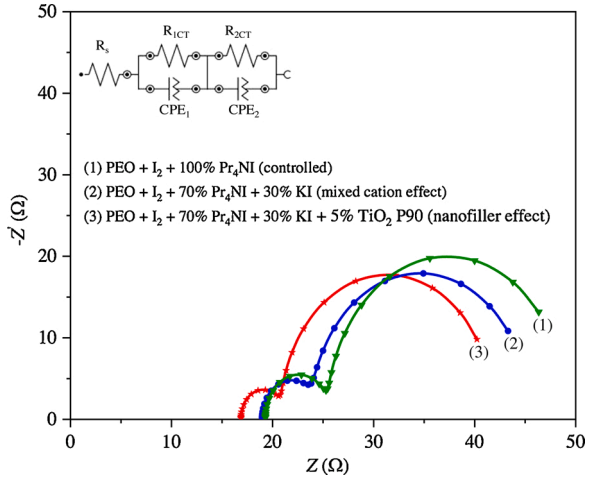

Fig. 13. Nyquist plots of solar cells with different electrolyte compositions under the simulated light of 100 mW cm^{-2} with AM 1.5 spectral filter.

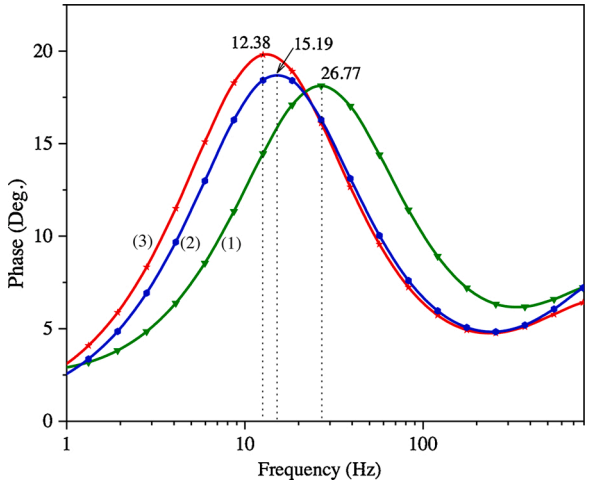

Fig. 14. Bode plots of solar cells with different electrolyte compositions under the illumination of 100 mW cm^{-2} with AM 1.5 spectral filter.

cell and best solar cells. CPE_1 and CPE_2 denote the constant phase elements. R_s is the series resistance, R_{1CT} is the charge transfer resistance and R_{2CT} is the recombination resistance. The best solar cell has a small charge transfer resistance and high recombination resistance than the controlled cell.

Fig. 14 shows the Bode phase plots of the solar cells with PbS/CdS/N719 photoanode and different compositions in the electrolyte. Peaks of the Bode plot are shifted towards the lower frequencies due to the mixed cation effect and nanofiller effects. In other words, electron lifetime in the TiO_2 nanostructure is increased. Lifetime of the electrons was estimated using the following equation:

$$\tau = \frac{1}{2\,\pi\, f_{max}}$$

where f_{max} is the frequency corresponding to the maximum phase angle.

Electrochemical impedance spectroscopy parameters of the controlled and best solar cells are listed in Table 9. Solar cell fabricated with mixed salt and nanofiller based polymer electrolyte shows lowest series resistance of 16.9 Ω and charge transfer resistance of 3.94 Ω, which leads an efficient electron transfer and enhances the short-circuit current density of the solar cell. Nanofiller incorporated electrolyte based solar cells show a longer electron lifetime of 12.86 ms with less recombination. This clearly confirms that the electrons are effectively transferred and photocurrent is enhanced [57,58].

In the present study, fabrication of the photoanodes and electrolytes are highly reproducible. Maximum error associated with the efficiency of the overall performance of the solar cell is 0.09.

4. Conclusion

In this work we have succeeded in applying the cumulative beneficial effects of (a) co-sensitization of the TiO_2 photoanode with PbS/CdS core-shell quantum dots and N719 dye, (b) incorporating a binary mixture of two iodide salts, Pr_4NI with a bulky cation and KI with a small cation in the plasticized, poly(ethylene oxide) (PEO) based solid polymer electrolyte to enhance the ionic conductivity and short circuit photocurrent by the novel "mixed cation effect", and (c) incorporating the TiO_2 nanofiller in the same electrolyte, to enhance the overall performance of the solar cells to achieve a significantly high energy conversion efficiency of 4.41 %.

Authorship contributions

Please indicate the specific contributions made by each author.

Conception and design of study: M.A.K.L. Dissanayake, G.K.R. Senadeera

Acquisition of data: T. Jaseetharan, J.M.K.W. Kumari

Analysis and interpretation of data: B-E. Mellander, I. Albinsson, M. Furlani

Drafting the manuscript: T. Jaseetharan, J.M.K.W. Kumari

Revising the manuscript critically for important intellectual content: : M.A.K.L. Dissanayake, G.K.R. Senadeera

Approval of the version of the manuscript to be published (the names of all authors must be listed):

Table 9
EIS parameters of solar cells with different electrolyte compositions.

Optimized compositions of solid polymer electrolyte	R_S (Ω)	R_{1CT} (Ω)	R_{2CT} (Ω)	J_{sc} (mA cm^{-2})	τ (ms)
(1) PEO + I_2 + 100% Pr_4NI (reference)	19.3	6.18	21.7	6.380	5.95
(2) PEO + I_2 + 70% Pr_4NI + 30% KI	19.0	4.98	24.4	7.996	10.48
(3) PEO + I_2 + 70% Pr_4NI + 30% KI + 5% TiO_2 P90	16.9	3.94	26.2	8.412	12.86

M.A.K.L. Dissanayake, T. Jaseetharan, G.K.R. Senadeera, B-E. Mellander, I. Albinsson, M. Furlani, J.M.K.W. Kumari

Declaration of Competing Interest

The authors declare that they have no known competing financial interests or personal relationships that could have appeared to influence the work reported in this paper.

Acknowledgements

This research work received financial support from the National Science Foundation of Sri Lanka under grant number NSF/SCH/2018/04.

Appendix A. Supplementary data

Supplementary material related to this article can be found, in the online version, at doi:https://doi.org/10.1016/j.jphotochem.2020.112915.

References

[1] M. Grätzel, Dye-sensitized solar cells, J. Photochem. Photobio. C Photochem Rev. 4 (2003) 145–153.
[2] D. Cahen, G. Hodes, M. Grätzel, J.F. Guillemoles, I. Riess, Nature of photovoltaic action in dye-sensitized solar cells, J. Phys. Chem. B 104 (9) (2000) 2053–2059.
[3] P. Tiwana, P. Docampo, M.B. Johnston, H.J. Snaith, L.M. Herz, Electron mobility and injection dynamics in mesoporous ZnO, SnO_2, and TiO_2 films used in dye-sensitized solar cells, ACS Nano 5 (6) (2011) 5158–5166.
[4] Q. Zhang, C.S. Dandeneau, X. Zhou, G. Cao, ZnO Nanostructures for dye-sensitized solar cells, Adv. Mater. 21 (2009) 4087–4108.
[5] T. Inoue, S.S. Pandey, N. Fujikawa, Y. Yamaguchi, S. Hayase, Synthesis and characterization of squaric acid based NIR dyes for their application towards dye-sensitized solar cells, J. Photochem. Photobio. A Chem. 213 (2010) 23–29.
[6] K. Kakiage, Y. Aoyama, T. Yano, K. Oya, J. Fujisawab, M. Hanaya, Highly-efficient dye-sensitized solar cells with collaborative sensitization by silyl-anchor and carboxy-anchor dyes, Chem. Commun. 51 (2015) 15894–15897.
[7] C.-M. Lan, H.-P. Wu, T.-Y. Pan, C.-W. Chang, W.-S. Chao, C.-T. Chen, C.-Li. Wang, C.-Y. Lin, E.W.-G. Diau, Enhanced photovoltaic performance with co-sensitization of porphyrin and an organic dye in dye-sensitized solar cells, Energy Environ. Sci. 5 (2012) 6460–6464.
[8] Y. Chen, Z. Zeng, C. Li, W. Wang, X. Wang, B. Zhang, Highly efficient co-sensitization of nanocrystalline TiO_2 electrodes with plural organic dyes, New J. Chem. 29 (2005) 773–776.
[9] D. Bera, L. Qian, T.-K. Tseng, P.H. Holloway, Quantum dots and their multimodal applications: a review, Materials 3 (2010) 2260–2345.
[10] J. Li, L. Zhao, S. Wanga, J. Hu, B. Dong, H. Lu, L. Wana, P. Wang, Great improvement of photoelectric property from co-sensitization of TiO_2 electrodes with CdS quantum dots and dye N719 in dye-sensitized solar cells, J. Mat. Res. Bull. 48 (2013) 2566–2570.
[11] Y. Liu, J. Wang, Co-sensitization of TiO_2 by PbS quantum dots and dye N719 in dye-sensitized solar cells, Thin Solid Films 518 (2010) 54–56.
[12] S. Luo, H. Shen, W. Hu, Z. Yao, J. Li, D. Oron, N. Wang, H. Lin, Improved charge separation and transport efficiency in panchromatic sensitized solar cells with co-sensitization of PbS/CdS/ZnS quantum dots and dye molecules, RSC Adv. 6 (2016) 21156–21164.
[13] A.K. Pandey, M.S. Ahmad, M. Alizadeh, N.A. Rahim, Improved electron density through Hetero-junction binary sensitized TiO_2/ CdTe / D719 system as photoanode for dye sensitized solar cell, Physica E Low. Syst. Nanostruct. 101 (2018) 139–143.
[14] A. Carella, R. Centore, F. Borbone, M. Toscanesi, M. Trifuoggi, F. Bella, C. Gerbaldi, S. Galliano, E. Schiavo, A. Massaro, A.B. Muñoz-García, M. Pavone, Tuning optical and electronic properties in novel carbazole photosensitizers for p-type dye-sensitized solar cells, Electrochim. Acta 292 (2018) 805–816.
[15] H.F. Etefa, T. Imae, M. Yanagida, Enhanced photosensitization by carbon dots co-adsorbing with dye on p-type semiconductor (nickel oxide) solar cells, ACS Appl. Mater. Interfaces 12 (2020) 18596–18608.
[16] B. Li, L. Wang, B. Kang, P. Wang, Y. Qiu, Review of recent progress in solid-state dye-sensitized solar cells, Sol. Energy Mater. Sol. Cells 90 (2006) 549–573.
[17] F. Bella, S. Galliano, G. Piana, G. Giacona, G. Viscardi, M. Gratzel, C. Barolo, C. Gerbaldi, Boosting the efficiency of aqueous solar cells: a photoelectrochemical estimation on the effectiveness of $TiCl_4$ treatment, Electrochim. Acta 302 (2019) 31–37.
[18] F. Bella, L. Porcarelli, D. Mantione, C. Gerbaldi, C. Barolo, M. Gratzel, D. Mecerreyes, A water-based and metal-free dye solar cell exceeding 7% efficiency using a cationic poly(3,4-ethylenedioxythiophene) derivative, Chem. Sci. 11 (2020) 1485–1493.
[19] P. Wang, S.M. Zakeeruddin, J.E. Moser, M.K. Nazeeruddin, T. Sekiguchi, M. Grätzel, A stable quasi-solid-state dye-sensitized solar cell with an amphiphilic ruthenium sensitizer and polymer gel electrolyte, Nat. Mater. 2 (2003) 402–407.
[20] C.-L. Chen, T.-W. Chang, H. Teng, C.-G. Wu, C.-Y. Chen, Y.-M. Yanga, Y.-L. Lee, Highly efficient gel-state dye-sensitized solar cells prepared using poly (acrylonitrile-co-vinyl acetate) based polymer electrolytes, Chemphyschem 15 (2013) 3640–3645.
[21] J. Wu, Z. Lan, J. Lin, M. Huang, S. Hao, T. Sato, S. Yin, A Novel thermosetting gel electrolyte for stable quasi-solid-state dye-sensitized solar cells, Adv. Mater. 19 (2007) 4006–4011.
[22] G.K.R. Senadeera, S. Kobayashi, T. Kitamura, Y. Wada, S. Yanagida, Versatile preparation method for mesoporous TiO_2 electrodes suitable for solid-state dye sensitized photocells, Bull. Mater. Sci. 28 (6) (2005) 635–641.
[23] K. Tennakone, G.R.R.A. Kumara, A.R. Kumarasinghe, G.U. Wijayantha, P. M. Sirimanne, A dye-sensitized nano-porous solid-state photovoltaic cell, Semicond. Sd. Technol. 10 (1995) 1689–1693.
[24] F. Fabregat-Santiago, J. Bisquert, L. Cevey, P. Chen, M. Wang, S.M. Zakeeruddin, M. Gratzel, Electron transport and recombination in solid-state dye solar cell with spiro-OMeTAD as hole conductor, J. Am. Chem. Soc. 131 (2009) 558–562.
[25] M.R. Johan, O.H. Shy, S. Ibrahim, S.M.M. Yassin, T.Y. Hui, Effects of Al_2O_3 nanofiller and EC plasticizer on the ionic conductivity enhancement of solid PEO–$LiCF_3SO_3$ solid polymer electrolyte, Solid State Ion. 196 (2011) 41–47.
[26] H. Han, W. Liu, J. Zhang, X.-Z. Zhao, A hybrid poly(ethylene oxide)/ poly (vinylidene fluoride)/TiO_2 nanoparticle solid-state redox electrolyte for dye-sensitized nanocrystalline solar cells, Adv. Fun. Matter. 15 (12) (2005) 1940–1944.
[27] M.-S. Kang, J.H. Kim, Y.J. Kim, J. Won, N.-G. Parkc, Y.S. Kang, Dye-sensitized solar cells based on composite solid polymer electrolytes, Chem. Commun. 889- (2005) 891.
[28] K. Sundaramoorthy, S.P. Muthu, R. Perumalsamy, Enhanced performance of 4,4′-bipyridine-doped PVDF/KI/I2 based solid state polymer electrolyte for dye-sensitized solar cell applications, J. Mat. Sci. Mat. Electron. 29 (21) (2018) 18074–18081.
[29] H. Jauhari, R. Grover, N. Gupta, O. Nanda, D.S. Mehta, K. Saxena, Solid state dye sensitized solar cells with polyaniline- polyanilinethiourea based polymer electrolyte composition, J. Ren. Sust. Energy 10 (2018), 033502.
[30] Y. Duan, Q. Tang, Y. Chen, Z. Zhao, Y. Lv, M. Hou, P. Yang, B. He, L. Yu, Solid-state dye-sensitized solar cells from poly(ethylene oxide)/polyaniline electrolytes with catalytic and hole-transporting characteristics, J. Mater. Chem. A 3 (2015) 5368–5374.
[31] B. Bhattacharya, J.Y. Lee, J. Geng, H.-T. Jung, J.-K. Park, Effect of cation size on solid polymer electrolyte based, dye-sensitized solar cells, Langmuir 25 (2009) 3276–3281.
[32] M.A.K.L. Dissanayake, C.A. Thotawatthage, G.K.R. Senadeera, T.M.W.J. Bandara, W.J.M.J. Jayasundera, B.-E. Mellander, Efficiency enhancement by mixed cation effect in dye-sensitized solar cells with PAN based gel polymer electrolyte, J. Photochem. Photobio. A Chem. 246 (2012) 29–35.
[33] A.K. Arof, M.F. Aziz, M.M. Noor, M.A. Careem, L.R.A.K. Bandara, C. A. Thotawatthage, W.N.S. Rupasinghe, M.A.K.L. Dissanayake, Efficiency enhancement by mixed cation effect in dye-sensitized solar cells with a PVdF based gel polymer electrolyte, Int. J. Hydrogen Energy 39 (6) (2014) 2929–2935.
[34] C.C. Tambelli, A.C. Bloise, A.V. Rosario, E.C. Pereira, C.J. Magon, J.P. Donoso, Characterisation of PEO-Al_2O_3 composite polymer electrolytes, Electrochim. Acta 47 (2002) 1677–1682.
[35] S. Anandan, R. Sivakumar, Effect of loaded TiO_2 nanofiller, on heteropolyacid-impregnated PVDF polymer electrolyte for the performance of dye-sensitized solar cells, Phys. Status Solidi A 206 (2) (2009) 343–350.
[36] M.A.K.L. Dissanayake, W.N.S. Rupasinghe, V.A. Seneviratne, C.A. Thotawatthage, G.K.R. Senadeera, Optimization of iodide ion conductivity and nano filler effect for efficiency enhancement in polyethylene oxide (PEO) based dye sensitized solar cells, Electrochim. Acta 145 (2014) 319–326.
[37] J. Duan, H. Zhang, Q. Tang, B. Heb, L. Yu, Recent advances in critical materials for quantum dot-sensitized solar cells: a review, J. Mater. Chem. A 3 (2015) 17497–17510.
[38] M. Shalom, J. Albero, Z. Tachan, E. Martínez-Ferrero, A. Zaban, E. Palomares, Quantum dot-dye bilayer-sensitized solar cells: breaking the limits imposed by the low absorbance of dye monolayers, J. Phys. Chem. Lett. 1 (2010) 1134–1138.
[39] B. Wang, H. Ding, Y. Hu, H. Zhou, S. Wang, T. Wang, R. Liu, J. Zhang, X. Wang, H. Wang, Power conversion efficiency enhancement of various size CdS quantum dots and dye co-sensitized solar cells, Int. J. Hydrogen Energy 38 (36) (2013) 16733–16739.
[40] I. Moreels, Y. Justo, B. De Geyter, K. Haustraete, J.C. Martins, Z. Hens, Size-tunable, bright, and stable PbS quantum dots: a surface chemistry study, ACS Nano 5 (3) (2011) 2004–2012.
[41] A.M. Erkabaeva, T.V. Yaroslavtseva, S.E. Popov, O.V. Bushkova, FTIR and quantum chemical study of LiBr solvation in acetonitrile solutions, Vib. Spectrosc. 75 (2014) 19–25.
[42] J. Barthel, R. Deser, FTIR study of ion solvation and ion-pair formation in alkaline and alkaline earth metal salt solutions in acetonitrile, J. Sol. Chem. 23 (10) (1994) 1133–1146.
[43] M.J. Reddy, P.P. Chu, Optical microscopy and conductivity of poly(ethylene oxide) complexed with KI salt, Electrochim. Acta 47 (2002) 1189–1196.
[44] M.J. Reddy, P.P. Chu, Effect of Mg^{2+} on PEO morphology and conductivity, Solid State Ion. 149 (2002) 115–123.
[45] A.R. Polu, D.K. Kim, H.-W. Rhee, Poly(ethyleneoxide)-lithium difluoro(oxalato) borate new solid polymer electrolytes: ion–polymer interaction, structural, thermal, and ionic conductivity studies, Ionics 21 (10) (2015) 2771–2780.

[46] N. Zebardastan, M.H. Khanmirzaei, S. Ramesh, K. Ramesh, Novel poly(vinylidene fluoride-co-hexafluoro propylene)/polyethylene oxide based gel polymer electrolyte containing fumed silica (SiO_2) nanofiller for high performance dye-sensitized solar cell, Electrochim. Acta 220 (2016) 573–580.
[47] B. Muthuraamana, G. Will, H. Wanga, P. Mooniea, J. Bell, Increased charge transfer of Poly (ethylene oxide) based electrolyte by addition of small molecule and its application in dye-sensitized solar cells, Electrochim. Acta 87 (2013) 526–531.
[48] P.P. Chu, M.J. Reddy, H.M. Kao, Novel composite polymer electrolyte comprising mesoporous structured SiO_2 and PEO/Li, Solid State Ion. 156 (2003) 141–153.
[49] S. Das, A. Ghosh, Ionic conductivity and dielectric permittivity of PEO-$LiClO_4$ solid polymer electrolyte plasticized with propylene carbonate, AIP Adv. 5 (2015), 027125.
[50] A. Karmakar, A. Ghosh, Poly ethylene oxide (PEO)–LiI polymer electrolytes embedded with CdO nanoparticles, J. Nanopart. Res. 13 (2011) 2989–2996.
[51] G.P. Kalaignan, M.-S. Kang, Y.S. Kang, Effects of compositions on properties of PEO–KI–I_2 salts polymer electrolytes for DSSC, Solid State Ion. 177 (2006) 1091–1097.
[52] A. Dey, S. Karan, S.K. De, Effect of nanofillers on thermal and transport properties of potassium iodide_polyethylene oxide solid polymer electrolyte, Solid State Comm. 149 (2009) 1282–1287.
[53] M.A.K.L. Dissanayake, E.M.B.S. Ekanayake, L.R.K. Bandara, V.A. Seneviratne, C. A. Thotawatthage, S.L. Jayaratne, G.K.R. Senadeera, Efficiency enhancement by mixed cation effect in polyethylene oxide (PEO)-based dye-sensitized solar cells, J. Solid State Electrochem. 20 (1) (2016) 193–201.
[54] R. Nadimicherla, R. Kalla, R. Muchakayala, X. Guo, Effects of potassium iodide (KI) on crystallinity, thermal stability, and electrical properties of polymer blend electrolytes (PVC/PEO:KI), Solid State Ion. 278 (2015) 260–267.
[55] T.M.W.J. Bandara, D.G.N. Karunathilaka, J.L. Ratnasekera, L.A. De Silva, A. C. Herath, B.-E. Mellander, Electrical and complex dielectric behaviour of composite polymer electrolyte based on PEO, alumina and tetrapropyl ammonium iodide, Ionics 23 (7) (2017) 1711–1719.
[56] Y. Liu, J.Y. Lee, L. Hong, Morphology, crystallinity, and electrochemical properties of in situ formed poly (ethylene oxide)/TiO_2 nanocomposite polymer electrolytes, J. Appl. Polym. Sci. 89 (2003) 2815–2822.
[57] M.A.K.L. Dissanayake, T. Jaseetharan, G.K.R. Senadeera, J.M.K.W. Kumari, C. A. Thotawatthage, B.-E. Mellander, I. Albinson, M. Furlani, Highly efficient, PbS: Hg quantum dot-sensitized, plasmonic solar cells with TiO_2 triple-layer photoanode, J. Solid State Electrochem. 23 (6) (2019) 1787–1794.
[58] W. Wang, J. Du, Z. Ren, W. Peng, Z. Pan, X. Zhong, Improving loading amount and performance of quantum dot sensitized solar cells through metal salt solutions treatment on photoanode, ACS Appl. Mater. Interfaces 8 (45) (2016) 31006–31015.
[59] Woohyung Cho, Young Rae Kim, Donghoon Song, Hyung Woo Choi, Yong Soo Kang, High-efficiency solid-state polymer electrolyte dye-sensitized solar cells with a bi-functional porous layer, J. Mater. Chem. A (2) (2014) 17746–17750.
[60] Seckin Akin, Michael Bauer, Ryusuke Uchida, Neha Arora, Gwenole Jacopin, Yuhang Liu, Dirk Hertel, Klaus Meerholz, Elena Mena-Osteritz, Peter Bäuerle, Shaik Mohammed Zakeeruddin, M Ibrahim Dar, Michael Grätzel, ACS Appl. Energy Mater. 7 (2020) 6, https://doi.org/10.1021/acsaem.0c00811.